Haest, C. W. M., de Gier, J. van Es, G. A., Verkleij, A. J., & van Deenen, L. L. M. (1972) *Biochim. Biophys. Acta 288*, 43–53.
Hauser, H., & Gains, N. (1982) *Proc. Natl. Acad. Sci. U.S.A. 79*, 1683–1687.
Hauser, H., Gains, N., Eible, H.-J., Muller, M., & Wehrli, E. (1986) *Biochemistry 25*, 2126–2134.
Hope, M. J., Bally, M. B., Webb, G., & Cullis, P. R. (1985) *Biochim. Biophys. Acta 812*, 55–65.
Huang, C. H. (1969) *Biochemistry 8*, 344–352.
Ladbrooke, B. D., & Chapman, D. (1969) *Chem. Phys. Lipids 3*, 304–364.
Lentz, B. R., Alford, D. R., & Dombrose, F. A. (1980) *Biochemistry 19*, 2555–2559.
Li, W., & Haines, T. H. (1986) *Biochemistry 25*, 7477–7483.
Linden, C. D., Wright, K. L., McConnell, H. M., & Fox, C. F. (1973) *Proc. Natl. Acad. Sci. U.S.A. 70*, 2271–2275.
Mayer, L. M., Hope, M. J., & Cullis, P. R. (1986) *Biochim. Biophys. Acta 858*, 161–168.
Michaelson, D. M., Horwitz, A. F., & Klein, M. P. (1973) *Biochemistry 12*, 2637–2645.
Nordlund, J. R., Schmidt, C. F., & Thompson, T. E. (1981) *Biochemistry 20*, 6415–6420.
Op den Kamp, J. A. F., de Gier, J., & van Deenen, L. L. M. (1974) *Biochim. Biophys. Acta 345*, 253–256.
Op den Kamp, J. A. F., Kauerz, M. Th., & van Deenen, L. L. M. (1975) *Biochim. Biophys. Acta 406*, 169–177.
Papahadjopoulos, D., Jacobsen, K., Niz, S., & Isac, T. (1973) *Biochim. Biophys. Acta 345*, 253–256.
Vail, W. J., & Stollery, J. G. (1979) *Biochim. Biophys. Acta 551*, 74–84.
van Dijck, P. W. M., Ververgaert, P. M. J. T., van Deenen, L. L. M., & de Gier, J. (1975) *Biochim. Biophys. Acta 406*, 465–478.
van Dijck, P. W. M., de Kruijff, B., Verkleij, A. J., van Deenen, L. L. M., & de Gier, J. (1978) *Biochim. Biophys. Acta 512*, 84–96.

Molecular Topography of Toxic Shock Syndrome Toxin 1 As Revealed by Spectroscopic Studies†

Bal Ram Singh, Nighat P. Kokan-Moore,‡ and Merlin S. Bergdoll*
Food Research Institute, University of Wisconsin—Madison, Madison, Wisconsin 53706
Received March 31, 1988; Revised Manuscript Received July 8, 1988

ABSTRACT: Molecular characterization of toxic shock syndrome toxin 1 has been carried out and compared with a group of functionally related staphylococcal enterotoxins. The secondary structure analysis of the far-UV circular dichroic spectrum of toxic shock syndrome toxin 1 revealed 6.25% α-helix, 51.25% β-pleated sheets, 9.0% β-turns, and 33.5% random coils. The pattern, in general, was similar to the staphylococcal enterotoxins. Four antigenic sites have been predicted for toxic shock syndrome toxin 1 by using the secondary structure information in combination with the hydrophilicity calculation. The location of the antigenic sites, in general, agrees with the experimental results. Topographical analysis of the tyrosine residues as determined by second-derivative UV spectroscopy [Ragone, R., Colonna, G., Balestrieri, C., Servillo, L., & Irace, G. (1984) *Biochemistry 23*, 1871–1875] showed that six of nine tyrosine residues are exposed to aqueous solvent. Tryptophan fluorescence quenching studies with an anionic surface quencher, I^-, and a neutral quencher, acrylamide, revealed that almost all of the tryptophan residues are buried in the protein matrix as their accessibility to the surface quencher is very low (17%). Since there are only three tryptophan residues in the amino acid sequence of the toxic shock syndrome toxin 1 and there is a tyrosine residue (Tyr-15, Tyr-115, and Tyr-153) next to each of the tryptophan residues (Trp-14, Trp-116, and Trp-154), it appears the tyrosine residues not exposed to the aqueous solvent are those next to the tryptophan residues. Functional implications of the topography of the tryptophan and tyrosine residues are assessed.

Toxic shock syndrome toxin 1 (TSST-1) is recognized as the major toxin responsible for the signs and symptoms of toxic shock syndrome (TSS) (Bergdoll et al., 1981; Schlievert et al., 1981; de Azavedo & Arbuthnott, 1984; Rasheed et al., 1985). TSS elicits symptoms such as high fever, low blood pressure, rash, hypotension, dizziness, desquamation of the palms of the hands and soles of the feet, and involvement of other organ systems (Todd et al., 1978; Davis et al., 1980; Shands et al., 1980).

TSST-1 is a small molecular weight protein (22K) that has been purified and biochemically characterized (Reiser et al., 1983; Blomster-Hautamaa et al., 1986b). The amino acid sequence shows no significant homology with the staphylococcal enterotoxins, a family of functionally related toxins (Blomster-Hautamaa et al., 1986b; Betley & Mekalanos, 1988), nor does it show any serological cross-reactivity with the enterotoxins. These observations were unexpected in view of the similarity of many of the signs and symptoms produced

† This investigation was supported in part by Procter & Gamble Co., Personal Products of Johnson and Johnson, Kimberly-Clark Corp., Tambrands, Playtex International, Inc., and the College of Agricultural and Life Sciences of the University of Wisconsin–Madison.
* Address correspondence to this author.
‡ Present address: Department of Anatomy and Cellular Biology, Medical College of Wisconsin, 8701 Watertown Plank Rd., Milwaukee, WI 53226.

0006-2960/88/0427-8730$01.50/0

in both humans and animals by these toxins (Bergdoll, 1983; Quimby & Nguyen, 1985; Crass & Bergdoll, 1986a,b). Several biological activities are shared: nonspecific mitogenicity in T-lymphocytes, suppression of in vitro primary antibody response, enhancement of host susceptibility to lethal shock by endotoxin, and evocation of γ-interferon (Schlievert et al., 1981; Bergdoll, 1983; Clavano et al., 1984; Poindexter & Schlievert, 1986). Both TSST-1 and the enterotoxins are sensitive to acids, are resistant to tryptic digestion, and have similar amino acid compositions; however, TSST-1 is digestible by pepsin and lacks any cysteine residues which are instrumental in forming the "cysteine loop" in the enterotoxins (Bergdoll & Robbins, 1973). In view of functional similarity, one must assume that the active sites are maintained in TSST-1 through the secondary and tertiary structure levels. No study of the secondary and tertiary structures of TSST-1 TSST-1 has been reported.

In this paper, we report (1) a comparison of the secondary structure parameters of TSST-1, obtained from circular dichroism, with those of the enterotoxins, (2) the topographical characterization of tyrosine and tryptophan residues from second-derivative UV spectroscopy and intrinsic fluorescence quenching, respectively, and (3) the antigenic sites as predicted from the secondary structure information and the hydrophilicity (Hopp & Woods, 1982).

Materials and Methods

Materials. TSST-1 produced by *Staphylococcus aureus* strain FRI-1169 was purified, lyophilized, and stored at 4 °C (Reiser et al., 1983). The lyophilized TSST-1 was dissolved in the appropriate buffer and filtered through a 0.2-μm Acro disk filter (Gelman Sciences) to obtain an optically clear protein solution for spectroscopic analysis. L-Tryptophan was from Sigma Chemical Co. (St. Louis, MO), and ultrapure guanidine hydrochloride was from Schwarz/Mann (Cleveland, OH). The other chemicals used were of the highest grade available commercially. All the buffers and solutions were made with deionized distilled water.

Absorption Spectra. Absorption spectra were recorded on a Beckman DU-7 spectrophotometer (Beckman Instruments) at room temperature (23–25 °C). Second-derivative analysis of the UV spectra was obtained with the same spectrophotometer. Circular dichroic spectra were recorded at room temperature (23–25 °C) on a JASCO J-20A CD/ORD spectrophotometer with a recording speed of 2 cm/min and wavelength expansion of 10 nm/cm. Time constants and slit width were fixed at 4 s and 1 nm, respectively. The spectra were recorded in a 1-mm path-length quartz cuvette using a protein concentration of 0.2–0.4 mg/mL. Secondary structural parameters were calculated by using the mean residue ellipticity at 1-nm intervals between 240 and 195 nm (Chang et al., 1978). In this method, secondary structure parameters are computed based on a linear least-squares fit of 15 reference proteins of known structure from X-ray crystallography.

Topographical location of tyrosine residues (tyrosines on the surface vs those buried in the protein matrix) was investigated according to the equation of Ragone et al. (1984):

$$\alpha = \frac{\gamma_n - \gamma_a}{\gamma_u - \gamma_a} \quad (1)$$

where α is the degree of tyrosine exposure to the solvent, γ_n and γ_u are the derivative peak ratios (a/b; Figure 2) of TSST-1 in native and unfolded (with 6 M Gdn-HCl) states, respectively, and γ_a is the second-derivative peak ratio of free tyrosine and tryptophan residues in the same molar ratio as that in TSST-1. The tyrosine to tryptophan molar ratio was taken as 3.00 for TSST-1 on the basis of the amino acid composition (Blomster-Hautamaa et al., 1986b). γ_a was calculated by using the equation (Ragone et al., 1984):

$$\gamma_a = \frac{Ax + B}{Cx + 1} \quad (2)$$

where A, B, and C are constants and x is the molar ratio of tyrosine to tryptophan in TSST-1.

Fluorescence Spectra. Fluorescence spectra were recorded at room temperature on an SLM 8000 "smart" spectrofluorometer. The excitation wavelength used was 295 nm to excite preferentially tryptophan residues. The emission spectra were recorded between 310 and 410 nm. Excitation and emission resolutions were set at 2 and 4 nm, respectively. The spectrum processings were carried out by using an SLM spectrum PR 8002 processor provided by SLM Instrument, Inc.

Tryptophan fluorescence quenching was investigated by using an anionic surface quencher (I^-) and a neutral (hydrophobic) quencher (acrylamide). Stock solutions of the quenchers (5 M KI and 8 M acrylamide) were prepared in the same buffer as the one in which TSST-1 was dissolved. A small volume of a quencher (1–5 μL at one step with maximum accumulation of 19 μL) was added to 700 μL of TSST-1 solution. The TSST-1 concentration for fluorescence measurements was used such that A_{295} (the excitation wavelength) was less than 0.1. This was done to minimize the inner filter effect. The fluorescence quenching data were analyzed by using both the Stern–Volmer plot (Stern & Volmer, 1919)

$$F_0/F = 1 + K_{sv}[Q] \quad (3)$$

and the modified Stern–Volmer plot (Lehrer, 1971)

$$\frac{F_0}{\Delta F} = \frac{1}{f_{acc}} + \frac{1}{f_{acc}K_Q[Q]} \quad (4)$$

F_0 and F are the fluorescence intensities in the absence and presence of a given concentration of quencher, [Q]. ΔF is the difference in the fluorescence intensities between the proteins without any addition of quencher and with the addition of a given concentration of quencher. K_{sv} and K_Q are Stern–Volmer and effective quenching constants, respectively. f_{acc} is the fraction of maximum accessible tryptophan fluorescence. The tryptophan fluorescence quantum yield of TSST-1 was calculated by comparing the area of emission spectra of TSST-1 ($FA_{protein}$) and free L-tryptophan (FA_{Trp}), both having the same A_{295}. The fluorescence quantum yield of free L-tryptophan was used as 0.20 (Teale & Weber, 1957):

$$\text{quantum yield} = (FA_{protein}/FA_{Trp})0.20 \quad (5)$$

Results

Circular Dichroism. The far-UV circular dichroic (CD) spectrum of TSST-1 is shown in Figure 1. The spectrum shows a sharp negative maximum at 204 ± 1 nm with a strong shoulder at 223 nm. The mean residue ellipticity at the negative maximum (204 nm) was −7032 ± 305 deg·cm^2 dmol^{-1}. The secondary structure analysis of the far-UV CD spectrum revealed 6.25% α-helix, 51.25% β-pleated sheets, 9.00% β-turns, and 33.50% random coils (Table I). The secondary structure parameters predicted from the amino acid sequence (Chou & Fasman, 1978) were 14.1% α-helix, 18.4% β-pleated sheets, 57.6% β-turns, and 9.9% random coils.

Second-Derivative Spectroscopy. The UV absorption spectrum shows a maximum at 279 nm, whereas the second-derivative spectrum (between 280 and 300 nm) shows two negative maxima at 284.5 and 291.5 nm and two positive maxima at 288.5 and 295.5 nm (Figure 2). The a/b ratio

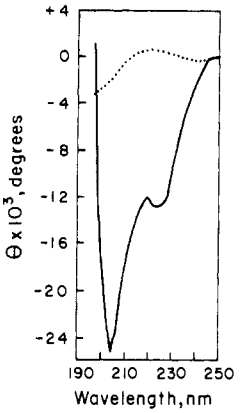

FIGURE 1: Far-UV CD spectrum (solid line) of toxic shock syndrome toxin 1 dissolved in 50 mM NaPB, pH 7.0, recorded at room temperature (23–25 °C) using a 1-mm path-length quartz cuvette. The concentration of protein used was 0.4 mg/mL. θ on the y axis represents the ellipticity in degrees. The base line (dotted line) was recorded for 50 mM NaPB, pH 7.0.

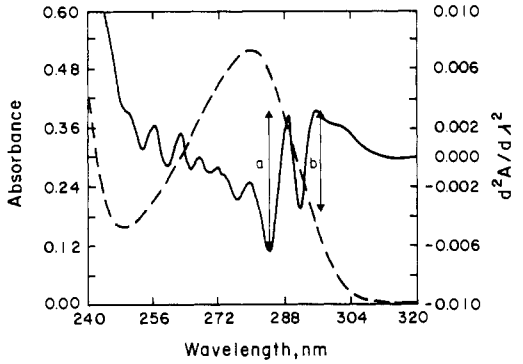

FIGURE 2: Absorption (dashed line) and second-derivative (solid line) spectra of toxic shock syndrome toxin 1 dissolved in 50 mM NaPB, pH 7.0. The absorption spectrum was recorded at 25 °C. The notation a represents the arithmetic sum of negative $d^2A/d\lambda^2$ of the peak at 284.5 nm and the positive $d^2A/d\lambda^2$ at 288.5 nm of the derivative spectrum. The notation b represents the arithmetic sum of the negative $d^2A/d\lambda^2$ of the peak at 291.5 nm and the positive $d^2A/d\lambda^2$ of the peak at 295.5 nm of the derivative spectrum.

Table I: Secondary Structure Analysis of Toxic Shock Sydrome Toxin 1 Derived from the Far UV Circular Dichroic Spectra between 240 and 195 nm and from the Amino Acid Sequence

secondary structure parameter	from	
	CD spectra	amino acid sequence[a]
α-helix (%)	6.25 ± 1.77	14.1
β-sheets (%)	51.25 ± 8.84	18.4
β-turns (%)	9.00 ± 6.36	57.6
random coils (%)	33.50 ± 0.71	9.9

[a] Chou and Fasman (1978) method.

in 50 mM NaPB, pH 7.0, was 1.364. The notation a represents the arithmetic sum of negative $d^2A/d\lambda^2$ of the peak at 284.5 nm and the positive $d^2A/d\lambda^2$ at 288.5 nm of the derivative spectrum. The notation b represents the arithmetic sum of the negative $d^2A/d\lambda^2$ of the peak at 291.5 nm and the positive $d^2A/d\lambda^2$ of the peak at 295.5 nm of the derivative spectrum. Treatment of TSST-1 with 6 M Gdn-HCl revealed negative maxima at 283.5 and 291 nm and positive maxima at 287.5 and 295.5 nm in its second derivative spectrum (spectrum not shown). The a/b ratio in 6 M Gdn-HCl was 1.952. The γ_a calculated according to eq 2 was 0.114. The degree of tyrosine exposure to the solvent was 66.5%. This corresponded to exposure of six of the nine tyrosine residues in TSST-1 to the aqueous solvent (Table II).

Table II: Degree of Tyrosine Exposure in Toxic Shock Syndrome Toxin 1 As Determined by Second-Derivative Spectroscopy

parameters	value	parameters	value
γ_n	1.364	α (%)	66.5
γ_u	1.952	no. of Tyr present	9.0
X	3.000	no. of Tyr exposed	6.0
γ_a	0.114		

Table III: Fluorescence Quenching Parameters, K_{sv}, K_Q, and f_{acc}, for I^- and Acrylamide Quenching of Tryptophan Fluorescence in Toxic Shock Syndrome Toxin 1

quencher	K_{sv} (M^{-1})	K_Q (M^{-1})	f_{acc}
I^-	0.96	11.73	0.17
acrylamide	2.20	2.12	1.04

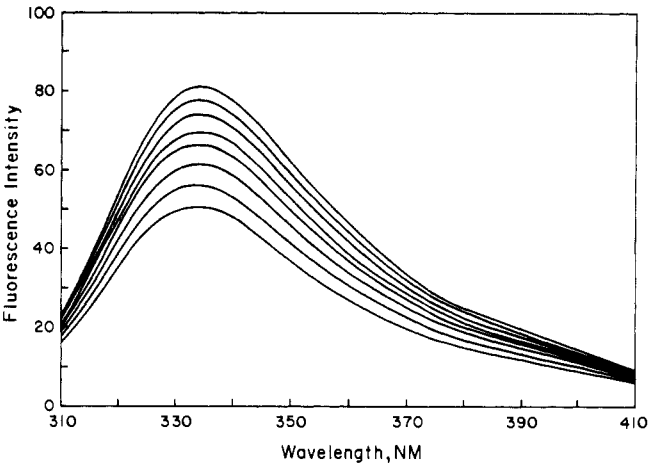

FIGURE 3: Tryptophan fluorescence spectra of toxic shock syndrome toxin 1 as a function of different concentrations of acrylamide. The protein and the stock solution of acrylamide were made in 50 mM NaPB, pH 7.0. Excitation wavelength was 295 nm, and the spectral resolutions on the excitation and emission monochromators were 2 and 4 nm, respectively. Acrylamide concentrations corresponding with spectra were 0 (top spectrum), 0.011, 0.034, 0.057, 0.079, 0.113, 0.157, and 0.211 M (bottom spectrum). All the spectral recordings were carried out at room temperature (23–25 °C).

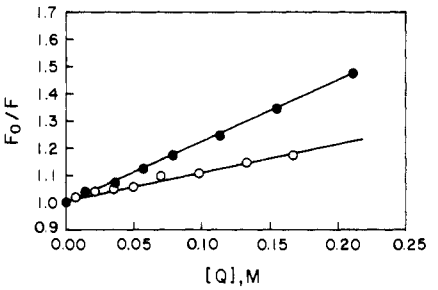

FIGURE 4: Stern–Volmer plots for the I^- (open circles) and acrylamide (closed circles) quenching of the tryptophan fluorescence of toxic shock syndrome toxin 1. For the details of fluorescence recordings, see Figure 3. F_0 and F are the tryptophan fluorescence intensities in the absence and presence, respectively, of an indicated concentration of the quencher, [Q] (I^- or acrylamide).

Fluorescence Spectroscopy. The intrinsic fluorescence was measured to probe the environment of tryptophan residues. The tryptophan emission maximum was observed at 333 nm (Figure 3), indicating that the fluorescent tryptophan residues are in a relatively hydrophobic environment. The tryptophan fluorescence quantum yield was estimated to be 0.24, the calculation based on the published absolute quantum yield of free L-tryptophan (Teale & Weber, 1957).

Tryptophan fluorescence quenching by a surface quencher (I^-) and a neutral quencher (acrylamide, a protein matrix penetrator; Eftink & Ghiron, 1984) was investigated to probe

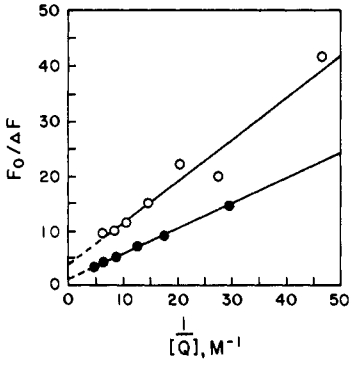

FIGURE 5: Modified Stern–Volmer plots for the I^- (open circles) and acrylamide (closed circles) quenching of the tryptophan fluorescence of toxic shock syndrome toxin 1. For the details of fluorescence recordings, see Figure 3. F_0 is the tryptophan fluorescence intensity in the absence of any quencher. ΔF is the difference in the tryptophan fluorescence intensity after the addition of an indicated concentration of the quencher, [Q] (I^- or acrylamide).

the specific environment around the fluorescent tryptophan residues. A representative set of emission spectra showing sequential quenching of tryptophan fluorescence by acrylamide is given in Figure 3. The Stern–Volmer plots for I^- and acrylamide quenching are shown in Figure 4. The slopes of these curves, Stern–Volmer constant (K_{sv}), were 0.96 and 2.20 M^{-1}, respectively, for I^- and acrylamide quenching (Table III). Modified Stern–Volmer plots of acrylamide and I^- quenching are shown in Figure 5. The effective quenching constants, K_Q, for acrylamide and I^- quenching were 2.12 and 11.73 M^{-1}, respectively, whereas the fractions of maximum fluorescent tryptophans accessible to acrylamide and I^- were 1.04 and 0.17, respectively (Table III).

Antigenic Determinants. Antigenic determinants were predicted according to the method of Hopp and Woods (1982) by calculating the hydrophilicity with a running indow of five amino acid residues (Figure 6B). Four antigenic sites were predicted for TSST-1, located at residues 57–78, 108–123, 145–151, and 172–180, with all of these sites occurring in segments which are predicted to be in a β-turn conformation (Hopp & Woods, 1982). The predicted secondary structure (Chou & Fasman method) along with the amino acid sequence is shown in Figure 6A.

Discussion

TSST-1 has several functional properties common to the staphylococcal enterotoxins even though there is no amino acid sequence homology between TSST-1 and the enterotoxins (Betley & Mekalanos, 1988). Is there a structural basis for this similarity in the biological functions of TSST-1 and the enterotoxins? The secondary structure parameters determined in this study partially answer the question.

TSST-1 has a very low content of α-helix and a relatively high content of β-sheet/β-turn structure. This, in general, agrees with these secondary structure parameters predicted from the amino acid sequence. The discrepancies in the predicted and experimental values for β-sheet and β-turns may be from the inherent inaccuracies involved in the methods used for determination of these structures (Chang et al., 1978; Chou & Fasman, 1978), especially with the program of Chang et al. (1978) which is weak in the determination of β-turns. Furthermore, only two or three amino acid residues were counted for β-turns by Chang et al. (1978), whereas in the method of Chou and Fasman (1978), tetrapeptides are counted in β-turns. It is notable that the sum of β-sheet and β-turns (Table I) determined experimentally (60.25% which could be

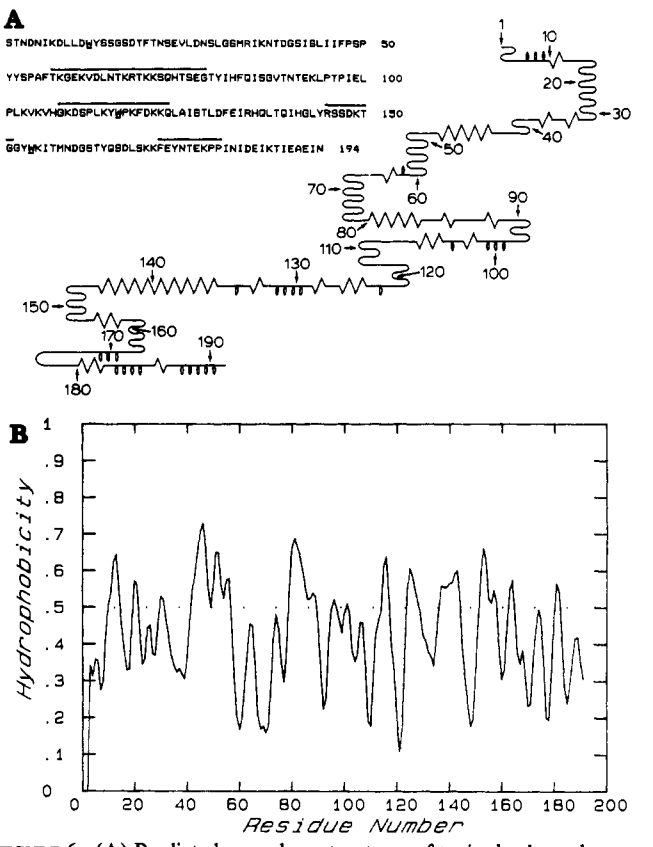

FIGURE 6: (A) Predicted secondary structures of toxic shock syndrome toxin 1 using a program developed by Black and Glorioso (1985). α-Helix, β-sheets, β-turns, and random coils are indicated by looped, jagged, wavy, and solid lines, respectively. The amino acid sequence of toxic shock syndrome toxin 1 (Blomster-Hautamaa et al., 1986) is shown also. The predicted antigenic sites are indicated by the overlines. (B) Zero-order hydrophobicity (inverted hydrophilicity) profile of toxic shock syndrome toxin 1 using the parameters of Hopp and Woods (1982) with a running window of five amino acid residues. Parameters are scaled to the range of 0–1 where 0 is the most hydrophilic (polar) and 1 is the most hydrophobic. The original hydrophilicity parameters (Y) can be obtained by using the equation $Y = (Z - 0.46875)/0.15625$ where X is the scale on the y axis of the plots.

75.45%, taking the deviations into account) is identical with the predicted sum of β-sheet and β-turns (76%), possibly owing to the explanation provided above. The low α-helical and high β-sheet/β-turn content has been found in staphylococcal enterotoxins A and E (Singh and Betley, unpublished data) and B and C_1 (Singh et al., 1988; Middlebrook et al., 1980). Although the primary structures are very different, TSST-1 maintains its secondary structure compatible to the enterotoxins. Such a similarity may explain how TSST-1 can share its biological activities with the enterotoxins.

The topographical location of tyrosine residues indicates that a large number of tyrosines (six of nine) are exposed to the aqueous solvent (Table II), implicating that they are on the surface of the proteins. It is interesting that three tyrosine residues in the primary structure of the TSST-1 (Blomster-Hautamaa et al., 1986b) are next to the three tryptophan residues (Trp-14, Trp-116, and Trp-154). Since the tryptophan residues are hydrophobic in nature, one could speculate that the three tyrosine residues which are not exposed to the surface are those next to tryptophan residues (i.e., Tyr-15, Tyr-115, and Tyr-153 are buried in the protein matrix). The surface topography of tyrosine and tryptophan residues is potentially important for locating the site for the biological activity. For example, an amino acid residue located at the

surface of a protein has potential to be involved in the binding with the putative receptor(s). Exposure of six of the nine tyrosine residues makes it likely that tyrosines play some role in the biological function of the TSST-1. Indeed, such was the case as the modification of tyrosine residues with tetranitromethane decreases the toxicity of the TSST-1 (Kokan, 1987).

The topography of tryptophan residues was investigated by intrinsic fluorescence quenching. The anionic quencher, I^-, had very little accessibility to the fluorescent tryptophan residues with only 17% of the fluorescent tryptophan residues being accessible to I^-. On the other hand, fluorescent tryptophan residues are readily accessible to a neutral quencher, acrylamide. This indicates that the tryptophan residues in TSST-1 are deeply buried in the inner foldings of the protein. Such a conclusion is drawn assuming that all the tryptophan residues are fluorescent. This assumption is supported by a relatively high tryptophan fluorescence quantum yield (0.24). The complete accessibility of tryptophan residues to only acrylamide also supports the conclusion that the tryptophan residues are in a hydrophobic environment as acrylamide is considered a hydrophobic quencher (Eftink & Ghiron, 1984). The comparison of quenching parameters for I^- and acrylamide quenching should be reflecting the true differences in the topography of the tryptophan residues as both the quenchers have quenching efficiencies of unity (Eftink & Ghiron, 1981) and thus the differences in parameters cannot be attributed to the differences in their quenching efficiency.

The conclusion that none of the tryptophan residues is accessible on the surface (vide supra) may indicate that they do not play much role at least in the binding of the toxin to the putative receptors. Incidentally, chemical modification of tryptophan residues does not affect the biological activity of TSST-1 (Kokan, 1987). Inaccessibility of all the tryptophan residues also supports indirectly the nonexposure of three tyrosine residues as determined by UV second-derivative spectroscopy (Table II).

The antigenic sites predicted with the secondary structure information in combination with the hydrophilicity indicate the strongest antigenic determinant to be located at residues 108–123 which agrees with the experimental result. Experimental results show the presence of a major antigenic site in the center 15-kDa segment of TSST-1 (Blomster-Hautamaa et al., 1986a; Kokan, 1987). In fact, two other predicted antigenic sites fall in the center 15-kDa segment (sites at residues 57–78 and 145–152). The accuracy of the predicted antigenic sites due to their occurrence in β-turns is quite logical because in each predicted antigenic site, two to four high β-turns forming amino acid residues (Pro, Gly, and Ser) are present (Blomster-Hautama et al., 1986b). None of the predicted antigenic determinant sequences of TSST-1 has any similarity with the predicted antigenic sequences of enterotoxins A, B, C_1, or E (to be published elsewhere).

In conclusion, the data presented here indicate the following: (1) the secondary structure of TSST-1 has low α-helix and high β-sheet/-turn contents, and this, in general, is similar to staphylococcal enterotoxins; (2) six of nine tyrosine residues are exposed on the surface of the protein; (3) the remaining three tyrosine residues that are likely to be buried in the protein matrix are Tyr-15, Tyr-115, and Tyr-153, each located next to three respective tryptophan residues, Trp-14, Trp-116, and Trp-154; (4) tryptophan residues are buried in the hydrophobic protein matrix; and (5) three major antigenic determinants are located on the center 15-kDa segment of TSST-1.

ACKNOWLEDGMENTS

We acknowledge the help of other members of the toxic shock syndrome team, Raoul F. Reiser, Ruth N. Robbins, and Amy C. Lee. We thank Dr. B. R. DasGupta for providing instrumental facilities to carry out CD and fluorescence studies.

Registry No. L-Trp, 73-22-3; L-Tyr, 60-18-4.

REFERENCES

Bergdoll, M. S. (1983) in *Staphylococci and Staphylococcal Infections* (Easmon, C. S. F., & Adlam, C., Eds.) pp 559–598, Academic, London.

Bergdoll, M. S., & Robbins, R. N. (1973) *J. Milk Food Technol. 36*, 610–612.

Bergdoll, M. S., Crass, B. A., Reiser, R. F., Robbins, R. N., & Davis, J. P. (1981) *Lancet 1*, 1017–1021.

Betley, M. J., & Mekalanos, F. J. (1988) *J. Bacteriol. 170*, 34–41.

Black, S. O., & Glorioso, J. C. (1985) *BioTechniques 4*, 448–460.

Blomster-Hautamaa, D. A., Novick, R. P., & Schlievert, P. M. (1986a) *J. Immunol. 137*, 3572–3576.

Blomster-Hautamaa, D. A., Kreiswirth, B. M., Kornblum, J. S., Novick, R. P., & Schlievert, P. M. (1986b) *J. Biol. Chem. 261*, 15783–15786.

Calvano, S. E., Quimby, F. W., Antonacci, A. C., Reiser, R. F., Bergdoll, M. S., & Dineen, P. (1984) *Clin. Immunol. Immunopathol. 33*, 99–110.

Chang, C. T., Wu, C. S. C., & Yang, J. T. (1978) *Anal. Biochem. 91*, 13–31.

Chou, P. Y., & Fasman, G. D. (1978) *Annu. Rev. Biochem. 47*, 251–276.

Crass, B. A., & Bergdoll, M. S. (1986a) *J. Infect. Dis. 153*, 918–926.

Crass, B. A., & Bergdoll, M. S. (1986b) *J. Clin. Microbiol. 23*, 1138–1139.

Davis, J. P., Chesney, P. J., Wand, P. J., LaVenturee, M., & the Investigating and Laboratory Team (1980) *N. Engl. J. Med. 303*, 1429–1435.

de Azavedo, J. C. S., & Arbuthnott, J. P. (1984) *Infect. Immun. 46*, 314–317.

Eftink, M. R., & Ghiron, C. A. (1981) *Anal. Biochem. 114*, 199–227.

Eftink, M. R., & Ghiron, C. A. (1984) *Biochemistry 23*, 3891–3899.

Hopp, T. P., & Woods, K. R. (1982) *Proc. Natl. Acad. Sci. U.S.A. 78*, 3824–3828.

Kokan, N. P. (1987) Ph.D. Dissertation, University of Wisconsin–Madison, Madison, WI.

Lehrer, S. S. (1971) *Biochemistry 10*, 3254–3267.

Middlebrook, J. L., Spero, L., & Argos, P. (1980) *Biochim. Biophys. Acta 621*, 233–240.

Poindexter, N. J., & Schlievert, P. M. (1986) *J. Infect. Dis. 153*, 772–779.

Quimby, F. W., & Ngyen, H. T. (1985) *CRC Crit. Rev. Microbiol. 12*, 1–44.

Ragone, R., Collona, G., Balestrieri, C., Servillo, L., & Irace, G. (1984) *Biochemistry 23*, 1871–1875.

Rasheed, J. K., Arko, R. J., Feeley, J. C., Chanfler, F. W., Thronsberry, C., Gibson, R. J., Cohen, M. L., Jeffries, C. D., & Broome, C. V. (1985) *Infect. Immun. 47*, 598–604.

Reiser, R. F., Robbins, R. N., Moleto, A., Khoe, G. P., & Bergdoll, M. S. (1983) *Biochemistry 22*, 3907–3912.

Schlievert, P. M., Shands, K. N., Dan, B. B., Schmidt, G. P., & Mishimura, R. D. (1981) *J. Infect. Dis. 143*, 509–516.

Shands, K. M., Schmid, G. P., Dan, B. B., Blum, D., Guidotti, R. J., Hargrett, M. T., Anderson, R. L., Hill, D. L., Broome, C. V., Band, J. D., & Fraser, D. W. (1980) *N. Engl. J. Med. 303*, 1436–1442.

Singh, B. R., Evenson, M. L., & Bergdoll, M. S. (1988) *Biochemistry* (following paper in this issue).

Stern, O., & Volmer, M. (1919) *Phys. Z. 20*, 183–188.

Teale, F. W., & Weber, G. (1957) *Biochem. J. 65*, 476–482.

Structural Analysis of Staphylococcal Enterotoxins B and C_1 Using Circular Dichroism and Fluorescence Spectroscopy†

Bal Ram Singh, Mary L. Evenson, and Merlin S. Bergdoll*

Food Research Institute, University of Wisconsin—Madison, Madison, Wisconsin 53706

Received April 1, 1988; Revised Manuscript Received July 8, 1988

ABSTRACT: Secondary and tertiary structural parameters of two functionally and serologically related proteins, staphylococcal enterotoxins B and C_1, have been determined by using circular dichroism and fluorescence spectroscopy. The secondary structures derived from the respective far-UV circular dichroic spectra were 9.5% α-helix, 55.0% β-pleated sheets, 16.5% β-turns, and 19.0% random coils for enterotoxin B and 15.0% α-helix, 38.0% β-pleated sheets, 25.5% β-turns, and 21.5% random coils for staphylococcal enterotoxin C_1. The values matched well with the secondary structures derived from the amino acid sequences (Chou and Fasman method). Seven antigenic sites have been predicted for both staphylococcal enterotoxins B and C_1 by using the hydrophilicity and the secondary structure information. Three of these antigenic sites appear similar. Fluorescence quantum yield of the single tryptophan residue (Trp-197) of both the enterotoxins showed the tryptophan residue in staphylococcal enterotoxin B to be ~46% more fluorescent than in staphylococcal enterotoxin C_1. Tryptophan fluorescence quenching by the surface quencher I^- and the neutral quencher acrylamide revealed that the single tryptophan residue in each of the enterotoxins is buried in the protein matrix and is not accessible to the surface quencher I^-. The tryptophan residue in staphylococcal enterotoxin C_1 is 14% less accessible to acrylamide than in staphylococcal enterotoxin B. The data, in general, reflect several similarities and significant differences between the two related enterotoxins.

The staphylococcal enterotoxins are a group of toxins that is responsible for bacterial food poisoning resulting in diarrhea and emesis. Staphylococcal enterotoxins B (SEB) and C_1 (SEC_1) have 239 amino acids each with molecular weights of 28.4K and 27.5K, respectively (Huang & Bergdoll, 1970; Schmidt & Spero, 1983). SEB and SEC_1 have significant serological cross-reactivity (Johnson et al., 1972; Spero et al., 1978) and a sequence homology of about 65% (Schmidt & Spero, 1983). Both toxins have a similar level of toxicity (Bergdoll, 1983). Clearly, a 35% difference in the amino acid sequence does not affect the biological activity of the toxins. Moreover, SEB and SEC_1 have significant differences in the nature of amino acids in their composition; SEB contains both more hydrophobic and more charged amino acids than SEC_1 (Huang & Bergdoll, 1970; Schmidt & Spero, 1983).

In order to establish a structural basis for their common biological action, secondary structure parameters for SEB and SEC_1 are derived from their respective far-UV circular dichroic (CD) spectra and compared with the predicted secondary structures based on the primary structure (Chou & Fasman, 1978). Probable antigenic sites are predicted by using the secondary structure information in conjunction with hydrophilicity. Secondary structures of SEB and SEC_1 were analyzed by Middlebrook et al. (1980). However, data were analyzed only for α-helices based on crude methods of Greenfield and Fasman (1969) and Chen et al. (1972). In this study, secondary structures were determined from the far-UV CD spectra by using the method of Chang et al. (1978) for α-helix, β-pleated sheets, β-turns, and random coils. In this method, the secondary structures are derived from a linear least-squares fit of the far-UV CD spectra of 15 reference proteins of known secondary structures.

Both SEB and SEC_1 have single tryptophan residues in their primary structure (Huang & Bergdoll, 1970; Schmidt & Spero, 1983) which are located at identical positions. This system is ideal for probing the topography of these tryptophan residues. Any differences in the microenvironments of the tryptophan residues should reflect differences in the protein folding (tertiary structure). Intrinsic fluorescence spectroscopy has been utilized to detect any differences in the surroundings of the single tryptophan residue each in SEB and SEC_1.

Materials and Methods

Materials. SEB and SEC_1 were purified and stored as lyophilized powders at 4 °C (Schantz et al., 1965; Borja & Bergdoll, 1967). Toxins were dissolved in 10 mM sodium phosphate buffer (NaPB), pH 7.2, just before use, and the protein solutions were filtered through 0.2-μm filters (Millipore) to get optically clear solutions. All the chemicals used were of the highest grade commercially available, and solutions and buffers were made with distilled water.

Absorption Spectra. Absorption measurements were made on a DU-7 spectrophotometer (Beckman Instruments). Far-UV circular dichroic spectra were recorded on a JASCO

† This work was supported in part by NIH Grant NS 17742 and DOD–University Research Instrumentation Award DAAG-29-83-G0063 to B. R. DasGupta and by the College of Agricultural and Life Sciences, University of Wisconsin–Madison.

* Address correspondence to this author.

0006-2960/88/0427-8735$01.50/0